Suggested Journal Section: Cellular & Molecular

LRRK2 controls synaptic vesicle storage and mobilization within the recycling pool

Condensed title: LRRK2 controls synaptic vesicle dynamics

Giovanni Piccoli[1], Steven B. Condliffe[2], Matthias Bauer[1,4], Florian Giesert[3], Karsten Boldt[1,5], Silvia De Astis[6], Andrea Meixner[1,5], Hakan Sarioglu[1], Daniela M. Vogt-Weisenhorn[3], Wolfgang Wurst[3], Christian Johannes Gloeckner[1], Michela Matteoli[6], Carlo Sala[2] and Marius Ueffing[1*]

[1]Department of Protein Science, Helmholtz Zentrum München

[2]IN-CNR, Milano

[3]Institute of Developmental Genetics, Helmholtz Zentrum München

[4]Department of Neurology, Hertie Institute for Clinical Brain Research, University of Tübingen, Tübingen, Germany

[5]Institute of Human Genetics, Klinikum rechts der Isar, Technical University of Munich

[6] Department of Medical Pharmacology, CNR Institute of Neuroscience and Fondazione Filarete, University of Milano

*to whom correspondence should be addressed: Marius Ueffing, Department of Protein Science, Helmholtz Zentrum München, German Research Center for Environmental Health, Ingolstaedter Landstr. 1, 85764 Neuherberg, phone: ++49-89-3187-3567 Fax: ++49-89-3187-4426, email: marius.ueffing@helmholtz-muenchen.de

Number of Figures and Tables: 8 figures, 1 table

Contents of Supplement Material: 1 table, 4 figures, 8 movies.

Number of Pages: 41

Word Count: Abstract – 143; Introduction – 408; Discussion - 1552.

Keywords: Parkinson's disease, LRRK2, endocytosis, EPSC, synaptic vesicle, interactome.

Acknowledgements: we thank Elisabeth Kremmer for producing monoclonal anti LRRK2 antibodies. The authors are grateful to Elöd Kortvély and Matteo Gorza for scientific discussions and critical reading of the manuscript and Luise Jennen for performing the electron microscopy. We thank Silke Becker and Sandra Helm for technical assistance on MS analysis and Martin Distel for his support on confocal microscopy. This work was supported by the National Genome Research Framework program NGFN-Plus, the Helmholtz Alliance for Mental Health in an Aging Society (HELMA) and the EU grant ProteomeBinders (FP6-026008). S.B.C was supported by CARIPLO grant "Brain on chip" Rif. 2006-0948. S.B.C. present address is Department of Physiology, Otago School of Medical Sciences, University of Otago, Dunedin, New Zealand

Abstract

Mutations in *Leucine-rich repeat kinase 2* (*LRRK2*) are the single most common cause of inherited Parkinson´s disease (PD). Little is known about its involvement in the pathogenesis of PD mainly due to the lack of knowledge about the physiological role of LRRK2. To determine the function of LRRK2, we studied the impact of shRNA-mediated silencing of LRRK2 expression in cortical neurons. Paired recording indicated that LRRK2 silencing affects evoked postsynaptic currents. Furthermore LRRK2 silencing induces at the presynaptic site a redistribution of vesicles within the bouton, altered recycling dynamics and increased vesicle kinetics. Accordingly, LRRK2 protein is present in the synaptosomal compartment of cortical neurons where it interacts with several proteins involved in vesicular recycling. Our results suggest that LRRK2 modulates synaptic vesicle trafficking and distribution in neurons and in consequence participates in regulating the dynamics between vesicle pools inside the presynaptic bouton.

Introduction

Parkinson's disease (PD) is a common neurodegenerative disease clinically characterized by bradykinesia, rigidity and resting tremor. A hallmark of the disease is the progressive loss of dopaminergic neurons in the substantia nigra and the formation of Lewy bodies (Moore et al., 2005; Hardy et al., 2006). Although the majority of cases are sporadic, mutations in the Leucine-rich repeat kinase 2 (LRRK2) gene (PARK8; OMIM 609007) are linked to late-onset autosomal dominant Parkinson's disease, accounting for up to 13% of familial PD cases compatible with dominant inheritance (Paisan-Ruiz et al., 2004; Zimprich et al., 2004) and 1 to 2% of sporadic PD patients, thus suggesting this protein as the most significant player in PD pathogenesis identified to date (Aasly et al., 2005; Berg et al., 2005; Taylor et al., 2006). The LRRK2 protein has a molecular weight of approximately 280 kDa and contains several domains including a Ras/GTPase like (Roc), a C-terminal of Roc (COR), a kinase (similar to mitogen activated protein kinase kinase kinases) and a WD40 domain (Bosgraaf and Van Haastert, 2003; Guo et al., 2006). Several single nucleotide alterations have been identified in LRRK2 (Brice, 2005), covering all functional domains, but only five missense mutations clearly segregate with PD in large family studies (Goldwurm et al., 2005; Bonifati, 2006). Some of these mutations cause increased kinase activity (West et al., 2005; Gloeckner et al., 2006; Greggio et al., 2006; Gloeckner et al., 2009).

Despite its predominance in PD, the physiological function of LRRK2 is not known, and therefore its precise role in the aetiology of PD is far from being understood, even though in vivo studies of mutant animals suggested an involvement in neurotransmitter release (Tong et al., 2009). Perturbations of LRRK2 expression have been shown to influence

neurite extension (MacLeod et al., 2006; Plowey et al., 2008; Wang et al., 2008; Gillardon, 2009) and vesicle endocytosis (Shin et al., 2008) .

In order to elucidate the physiological role of LRRK2, we determined the presynaptic and postsynaptic properties of cortical neurons in which LRRK2 had been silenced by short hairpin mediated RNA interference (Bauer et al., 2009). Electrophysiological analysis of such neurons revealed that LRRK2 silencing alters synaptic transmission. LRRK2 silencing perturbs vesicle dynamics and distribution within the recycling pool. On the molecular level, LRRK2 interacts with a number of proteins involved in synaptic vesicle trafficking. Taken together, our data suggests that LRRK2 participates in a protein network regulating synaptic vesicle trafficking in the presynaptic bouton.

Materials and methods

Lentiviral vector constructs, virus production and plasmids

Lrrk2 and Dlk1 target sequences were identified using Ambion-web-based oligo-search software and two sequences for LRRK2 (miB3: AAGTTGATAGTCAGGCTGAAT; miB4: AGTGCTCCGGTATCAGATG) and one for Dlk1 (miB5: AATGGAGTCTGCAAGGAAC) were selected, synthesized and cloned into GFP-expressing pLVTH as previously described (Bauer et al., 2008; Bauer et al., 2009). In brief, oligonucleotides (oligo-nt) coding for a 5'-pseudoBglII-site, a sense-oligo-nt-loop-antisense-oligo-nt, transcription termination site and a 3'pseudo-XbaI-restriction-site were purchased from Metabion. Sense and antisense oligos were annealed and subsequently phosphorylated. The fragments were cloned 3' to the H1-promoter of pBC KS+(ClaI)-H1, resulting in pBC KS+(ClaI)-sh. The H1sh cassettes were isolated with ClaI, blunted and cloned into the blunted ClaI/BamH1 site of pLV transfer-vector. pLV is a modified plasmid transfer vector derived from original pLVTH (Wiznerowicz and Trono, 2003), in which the BamH1-tetO-H1-ClaI fragment was excised. All recombinant lentiviruses were produced by transient transfection of HEK293T cells according to standard protocols (Wiznerowicz and Trono, 2003). Primary cortical cultures were transduced with LV vectors at multiplicity of infection 1 (MOI1). Empty virus (LVTH) has been used as control. For pull-down experiments, several hLRRK2 domains were subcloned into pDEST15 (N-GST tag) using Gateway system (Invitrogen): N-terminus (N-term., amino acids 1-397), ankyrin repeats (ANK, aa 394-995), leucine-rich repeats

(LRR, aa 921-1356), Roc-COR-Kinase domain (R-C-K, aa 1340-2142) and WD40 (aa 2124-2527).

Cortical neuron cultures, fractionation and chemicals

Cortical neuron cultures were prepared from embryonic day 17.5-18.5 (E17.5-18.5) mouse cortexes (CD1). High-density (750-1000 cells/mm^2) and medium-density (150–200 cells/mm^2) neuron cultures were plated and grown as described on 6-well plastic tissue culture plates (Iwaki; Bibby Sterilin Staffordshire, UK) or on 12 mm diameter coverslips put into 24-well plastic tissue culture plates (Iwaki; Bibby Sterilin Staffordshire, UK) (Romorini et al., 2004). Cells were infected with viruses at DIV10 and assayed as described throughout the text at DIV16-18. Subcellular fractions have been prepared as described (Dodd et al., 1981). Briefly high density cultures were collected in HEPES-buffered sucrose (0.32 M sucrose, 4 mM HEPES pH 7.4) and spun at 600g 4°C 5 minutes to pellet the nuclear fraction (P1). The resulting supernatant was centrifuged at 10.000g 4°C 15 minutes to obtain a cytosolic supernatant (S2) and a crude synaptosomal pellet that was lysed by hypoosmotic shock in 4 mM HEPES, pH 7.4. A final centrifugation step (at 25.000g 4°C 20 minutes) generated a supernatant (S3, crude synaptic vesicle fraction) and a pellet (P3, lysed synaptosomal membrane fraction). An equal amount of protein, as determined by Bradford assay (Biorad), was then separated on SDS-PAGE. Unless otherwise stated, all of the other chemicals came from Applichem, GmBH, Germany.

Pull-down, immuno-precipitation and antibodies

LRRK2 GST-fusion domains were expressed in E.Coli BL21 strain (Invitrogen), purified as described (Frangioni and Neel, 1993). 10 μg of each GST fusion protein was loaded on glutathion-sepharose resin (GE-Healthcare, Freiburg) and co-incubated with adult mouse brain lysate (1 mg of total protein). In immuno-precipitation assays, 10 mg of the indicated antibodies were incubated with 2 mg of adult mouse brain lysate and loaded on protein G-sepharose resin (GE-Healthcare, Freiburg). In both procedures, resins were extensively washed in Tris-EDTA buffer (10 mM Tris-HCl, pH 8.0, 1 mM EDTA,150 mM NaCl, 0.2% Triton-X100) and sample eluted with Laemmli buffer. For protein identification, samples were loaded onto 6-12% SDS-PAGE gels; the proteins were transferred onto nitrocellulose membrane (Sigma) at 80V for 120 minutes at 4°C. The primary antibodies were applied overnight in blocking buffer (20 mM Tris, pH 7.4, 150 mM NaCl, 0.1% Tween 20, and 5% non-fat dry milk); primary antibodies (source in parenthesis) included rat monoclonal anti-LRRK2 1E11 1:1000 (developed by Dr. E. Kremmer, Helmholtz Zentrum München), rabbit anti-PSD-95 1:1000 (gifts from E. Kim, KAIST); mouse anti-SNAP-25 1:1000 and rabbit anti-GluR2 1:250 (Chemicon); rabbit anti-NSF 1:1000, rabbit anti-HSP90 (Cell Signalling): rabbit anti-Vamp1 1:1000 (Synaptic System) mouse anti-syntaxin 1A 1:1000, mouse anti-synaptophysin 1:1000 and mouse anti-α-tubulin 1:1000 (Sigma). The secondary antibodies (HRP-conjugated anti-mouse, anti-rabbit or anti-rat) (Jackson ImmunoResearch) were used in a ratio of 1:2000. The signal was detected using an ECL detection system (GE-Healthcare, Freiburg) and quantified by means of ImageJ software (NIH).

MS/MS identification

LC-MSMS analysis was performed on an Ultimate3000 nano HPLC system (Dionex) online coupled to a LTQ OrbitrapXL (Thermo Fischer, Bremen, Germany) mass spectrometer by a nano spray ion source. The system was equipped with a nano trap column (100 µm i.d. × 2 cm, packed with Acclaim PepMap100 C18, 5 µm, 100 Å, LC Packings) and an analytical column (75 µm i.d. × 15 cm, Acclaim PepMap100 C18, 3 µm, 100 Å, LC Packings). Samples originating from pre-fractionation experiments were dissolved in 50 µl of 2% acetonitrile, 0.5% TFA by incubation for 15 minutes at 4°C under agitation. The samples were automatically injected and loaded onto the trap column at a flow rate of 30 µl/minute in 5% buffer B (80% acetonitrile, 0.1% FA in HPLC grade water) and 95% buffer A (5% acetonitrile, 0.1% FA in HPLC grade water). After 5 minutes the peptides were eluted and separated on the analytical column by a 140 min gradient from 5% to 40% of buffer B at 300 nl/minute flow rate. Remaining peptides were eluted by a short gradient from 50% to 100% buffer B in 5 minutes. The eluting peptides were ionized by nano spray ionization and the ionized peptides analyzed in the Orbitrap. From the MS prescan, the ten most intense peptide ions were selected for fragment analysis in the linear ion trap if they exceeded an intensity of at least 200 counts and if they were at least doubly charged. The normalized collision energy for CID was set to a value of 35 and the resulting fragments were detected with normal resolution in the linear ion trap. While the fragment analysis took place, a high resolution (60,000 FWHM) MS spectrum was acquired in the Orbitrap with a mass range from 200 to 1500 Da. The lock mass option was activated and a background signal with a mass of 445.120020 was used as lock mass (Olsen et al., 2005). Every ion selected for fragmentation, was

excluded for 30 seconds by dynamic exclusion. The acquired spectra were processed and analyzed either by using the Bioworks Browser software and the SEQUEST algorithm (Eng et al., 1994) for database searching . Monoisotopic masses and full tryptic cleavage were selected. The peptide tolerance was set to 10 ppm and the fragment ions tolerance to 1 Da. Only Y and Z ions were considered for the identification. The threshold for peak detection was set to 100 counts and the molecular weight range to 380-4500 Da. No fixed modifications and methionine oxidation, serine, threonine and tyrosine phosphorylation and cystein carbamidomethylation were allowed as variable modifications with a maximum of 3 modifications per peptide allowed. The database used was a mouse subset of the Uniref100 database (version 14.4, released on 2008-11-04).

Sequest result files were analyzed by the Scaffold software. Scaffold (version Scaffold_2_02_03, Proteome Software Inc., Portland, OR) was used to validate MS/MS based peptide and protein identifications. Peptide identifications were accepted if they could be established at greater than 95% probability as specified by the Peptide Prophet algorithm (Keller et al., 2002). Protein identifications were accepted if they could be established at greater than 99% probability and contained at least 2 identified unique peptides. Protein probabilities were assigned by the Protein Prophet algorithm (Nesvizhskii and Aebersold, 2004). Proteins that contained similar peptides and could not be differentiated based on MS/MS analysis alone were grouped to satisfy the principles of parsimony. Only hits confirmed by more then 2 independent experiments and absent in the GST control sample were taken in consideration.

Synaptotagmin antibodies uptake assay

The assay to monitor synapses recycling was performed using rabbit polyclonal antibodies directed against the intravesicular domain of synaptotagmin1 (Synaptic System), applied for 5 min if not indicated otherwise at RT on the cultures, as described previously (Matteoli et al., 1992). Incubations with the antibody (1:400) were performed in Tyrode solution containing 124 mM NaCl, 5 mM KCl, 2 mM $MgCl_2$, 30 mM glucose, 25 mM HEPES, pH 7.4 and 2mM $CaCl_2$ if not indicated otherwise or in Tyrode solution containing 50 mM KCl or 2 µm TTX or 0.5M sucrose. After fixation and permeabilization, a synaptophysin counter staining visualized the totality of synapses. Acquired images were processed and quantitatively analyzed with ImageJ software as previously described (Verderio et al., 1999). Briefly, GFP positive processes were manually tracked and the number of synaptotagmin and synaptophysin positive clusters and synaptophysin positive clusters present in the region of interest was automatically counted. To track synaptic vesicle movements, the neurons were incubated for 5 minutes with Cy3-coupled anti synaptotagmin 1 antibody (Synaptic System) in Tyrode solution at RT. The neurons were then washed, transferred to the microscope and imaged. Movies were acquired 2-5 minutes after labeling using a LSM Zeiss 510 confocal microscope equipped with a Zeiss 63X objective at 0.5 or 2 Hz sample frequency. Resulting images were optimized and processed on ImageJ. Single particle has been manually tracked using an algorithm implementation published by (Sbalzarini and Koumoutsakos, 2005). Briefly, images have been thresholded and circular ROI automatically generated around clusters. The position of the centre of each ROI along the time has been annotated. The diffusion coefficient D was calculated using the equation $MSD(\Delta t)=4D\Delta t$ where

MSD(Δt) indicates the mean square displacement of the single vesicle (Saxton, 1994). Only movies captured at 2 Hz sampling frequency have been included in the analysis and only particle tracks longer then 10 frames whose MSD(Δt) were consistent with the dynamic of spatial confined particles (Kusumi et al., 1993; Saxton, 1994) have been considered. At least three vesicles were analyzed for each experiment

Electron microscopy

Specimens from siLRRK2 and control infected neurons have been prepared for electron microscopy as described (Rudelius et al., 2006). Briefly, neuron cultures were fixed in cacodylate-buffered 3% glutaraldehyde for 12 h and subsequently Epon-embedded. Ultra-thin sections were cut, mounted on copper grids, contrasted with uranyl acetate and lead citrate and observed with an electron microscope (Zeiss EM10 at 60 kV).EM images have been processed on ImageJ (NIH) before performing the analysis on LoClust tool (Nikonenko and Skibo, 2004). Single vesicle has been manually annotated; only intact presynaptic boutons with similar size (longer then 300 nm and including more then 40 vesicles) have been included in the analysis. The n indicated through the text refers to presynaptic boutons measured.

Electrophysiology

Paired recordings were obtained from low density cultures of DIV14- to DIV16 neurons transfected at DIV10 bathed in an external solution [Krebs'—Ringer's–HEPES (KRH)] of the following composition: 125 mM NaCl, 5 mM KCl, 1.2 mM $MgSO_4$, 1.2 mM KH_2PO_4, 2 mM $CaCl_2$, 6 mM glucose and 25 mM HEPES, pH 7.4. Transfected

pyramidal neurons identified via positive GFP fluorescence were selected as the presynaptic neuron with an adjacent non-transfected pyramidal neuron serving as its post synaptic target. Both neurons were voltage clamped at -70 mV in the whole cell configuration using a MultiClamp 700A amplifier interfaced to a PC via a Digidata 1320 (Axon Instruments, CA) before depolarizing the presynaptic neuron with a single pulse (1ms, 100mV pulse) up to 30 mV while recording the response in the postsynaptic neuron as an evoked excitatory postsynaptic current (EPSC). Currents were sampled at 5-10 kHz and filtered at 5 kHz and data was acquired and analyzed offline using Clampfit 10 (Axon Instruments, CA). Average EPSCs were obtained by measuring consecutive EPSCs (n = 20 to 40) for each neuronal pair where events had to exceed a threshold of two to three times the SD of the baseline noise. Synaptic latency was calculated as the time spanning between the stimulus artifact and the 5% of EPSC amplitude (Markram et al., 1997; Bardoni et al., 2004). Spontaneous synaptic responses (mEPSCs) were monitored in medium density neuron cultures in the presence of 1 μM TTX. mEPSC amplitudes and frequencies were determined using Clampfit 10 software. Detection threshold for mEPSCs was set at 7–10 pA, depending on the amplitude of the membrane noise observed. Recording pipettes were fabricated from capillary glass using a two stage puller (Narishige, Tokyo, Japan) and had tip resistances of 3–5 MΩ when filled with the intracellular solution of the following composition: 130 mM K-gluconate, 10 mM KCl, 1 mM EGTA, 10 mM HEPES, 2 mM $MgCl_2$, 4 mM MgATP, and 0.3 mM Tris-GTP. Contaminating $GABA_A$-mediated responses were avoided by voltage-clamping neurons near the calculated equilibrium potential for Cl^- (-63 mV) under these conditions.

Statistical analysis

All data are expressed as mean ± standard error of the mean (SE). Data were analyzed with an unpaired Student's t test (two classes) or ANOVA followed by Tuckey's post hoc test (more than two classes). The indication of number of experiment (n) and level of significance (p) are indicated throughout the text.

Online supplemental material: Figure S1-4 provide additional confirmations for the evidences reported in the manuscript. Videos 1-8 report single vesicle dynamic in control and siLRRK2 neurons. Supplementary Table 1 lists further information related to protein identification.

Abbreviations: EPSC: evoked post synaptic currents, GFP: Green fluorescent protein, LRRK2: Leucine-rich repeat kinase 2, NSF: N-ethylmaleimide sensitive factor, RRP: ready releasable pool, RP: reserve pool, SV: synaptic vesicle, PD: Parkinson's disease

Results

LRRK2 is positively associated to neuron maturation

LRRK2 is widely expressed in neurons throughout the CNS, including cortex, striatum and other brain areas (Melrose et al., 2006; Higashi et al., 2007). As LRRK2 expression increases during postnatal development correlating with synaptic maturation (Biskup et al., 2007), we investigated LRRK2 protein expression in cortical neurons *in vitro* by western blotting at five different time points, DIV4, 8, 12, 16 and 20 that can be considered representative for neuron maturation (Lee and Sheng, 2000; Ziv and Garner, 2001). We detected LRRK2 by Western blot using a custom made rat monoclonal antibody (1E11) specific for LRRK2 (Bauer et al., 2009) (Figure 1A upper panel). As the predicted molecular weight (MW) of LRRK2 is about 286 kDa, we considered and analyzed the band at around 280 kDa as endogenous full length LRRK2. Interestingly, LRRK2 levels were positively associated with synapse maturation, as indicated by the increasing level of synaptophysin and PSD-95 proteins (Verderio et al., 1999; Buckby et al., 2004; Mielke et al., 2005) (Fig 1A-B). In contrast, no significant increase in tubulin was detected. This finding suggests a physiological role of LRRK2 in mature neurons.

LRRK2 silencing alters evoked postsynaptic currents

A recent publication proposed an involvement for LRRK2 in neurotransmitter release (Tong et al., 2009). Therefore, we tested if LRRK2 may modulate synaptic function. For these experiments and subsequent ones we impaired cellular LRRK2 expression via short hairpin mediated RNA interference. We infected cortical neurons with lentiviruses

expressing the silencing constructs on DIV10 and performed specific experimental procedures on DIV18. To test the efficiency of LRRK2 silencing, we infected mouse cortical neurons or NIH3T3 cells with control virus (LVTH) or with a virus expressing either the short hairpin construct miB3 or miB4, both of them specifically silencing LRRK2 (Bauer et al., 2009). miB3 siRNA mediated silencing led to an efficient reduction of the signal detected by the 1E11 antibody in cortical neurons (Figure 1C, miB3 lane) as well as in NIH3T3 cells (Supplementary Figure 1A). The same result was obtained when a second independent silencing construct (miB4) was transduced in cortical neurons (Figure 1C, miB4 lane). As both miB3 and miB4 constructs reduced LRRK2 protein expression to a similar extent (Figure 1D; LRRK2 protein levels, % of expression over control, mean±SE, LVTH=100±15.7, miB3=8.93±1.84, miB4=30.99±9.95; n=5, $p<0.01$), we mainly used miB3 for further experiments (hereinafter siLRRK2 while control refers to the LVTH virus). For the electrophysiological recordings, instead of infecting the cells with viruses, we transfected cortical neurons with a lentiviral plasmid construct. As the successful transfection of all constructs can be tracked via co-expressed GFP, we were able to identify transfected neurons as GFP positive cells. First we asked if LRRK2 might directly modulate neuron intrinsic excitability. To this purpose, we selected and patched non transfected or control or siLRRK2 transfected neurons surrounded by non transfected cells. When we recorded resting membrane potential and spontaneous miniature currents, we did not observe any obvious phenotype in siLRRK2 neurons (Supplementary figure 2A-C). Next we tested if LRRK2 silencing might affect presynaptic mechanism by measuring evoked EPSCs in pairs of synaptically connected pyramidal cortical neurons. Therefore, two adjacent neurons were chosen such that the presynaptic neuron was either

a lentiviral construct-control or a siLRRK2 transfected neuron whereas the postsynaptic neuron was always a non transfected cell (Supplementary figure 2D). The two neurons were whole cell voltage clamped at -70 mV and the presynaptic one was stimulated by a brief depolarization up to +30 mV generating an EPSC in the connected postsynaptic neuron. We first measured EPSCs after a single presynaptic stimulation (100mV, 1ms) in paired neurons (Figure 2A shows representative traces from control and siLRRK2 couples). We found that EPSC amplitude in postsynaptic neurons connected to siLRRK2 silenced presynaptic neurons (now referred to as siLRRK2 pairs) increased more than two fold compared to that measured in control pairs (Figure 2C,1st peak, EPSC amplitude [nA], mean±SE: control=-0.09±0.01, siLRRK2=-0.23±0.02, n=8, $p<0.001$). Furthermore, siLRRK2 pairs showed a higher probability to generate an EPSC over the baseline after a presynaptic trigger (percentage of successful events [%], mean±SE: control=84.63±2.66, siLRRK2=100±2, n=8, $p<0.001$). However, LRRK2 silencing did not significantly affect postsynaptic current latency and decay (Figure 2D, 1st peak and supplementary figure 2E). We next tested the impact of LRRK2 silencing after paired pulse stimulation (Matveev et al., 2002; Zucker and Regehr, 2002). Pairs of stimuli (100mV, 1ms) were elicited in the presynaptic cell at an interpulse interval of 50 ms (Figure 2B shows representative traces from control and siLRRK2 couples). In control pairs, the amplitude of the second EPSC was slightly increased, while LRRK2 silencing was associated with a robust impairment of the second EPSC (Figure 2C and supplementary figure 2F, EPSC2/EPSC1 [%] mean±SE: control=115.77±5.79, siLRRK2=55.44±2.39, n=5, $p<0.01$). Additionally, an increase in the latency of the second current was observed (Figure 2D, 2nd peak, postsynaptic current latency [ms], mean±SE: control=1.9±0.13,

siLRRK2=2.8±0.05, n=5, $p<0.01$). When we tried to rescue LRRK2 levels in siLRRK2 neurons by the means of LRRK2 over-expression, we observed cell death and we failed to record EPSC (data not shown). This might be due to the fact that LRRK2 overexpression in vitro is toxic (Greggio et al., 2006; Iaccarino et al., 2007; Li et al., 2010). Notwithstanding this, we believe these results suggest a role for LRRK2 in modulating presynaptic vesicle release.

LRRK2 silencing alters synaptic vesicle recycling

Given the electrophysiological changes associated with LRRK2 silencing, we asked if LRRK2 might be involved in presynaptic processes. We thus looked at the ratio of recycling synapses by exposing control and siLRRK2 infected cortical neuron cultures to anti synaptotagmin antibody as previously described (Matteoli et al., 1992; Bacci et al., 2001). These antibodies are internalized in the lumen of synaptic vesicles after their exo-endocytosis (Matteoli et al., 1992; Kraszewski et al., 1995; Malgaroli et al., 1995; Verderio et al., 1999), and their uptake closely reflects levels of vesicle recycling. Neurons were fixed after the given treatment and then putative synapses labeled post-fixation with synaptophysin antibodies. The synapses appeared as synaptotagmin and synaptophysin positive (i.e: recycling synapses) or only synaptophysin positive (i.e: not recycling synapses) clusters along GFP positive neuronal processes (Figure 3A and Supplementary Figure 3A). The analysis showed that under basal conditions (Figure 3B panel untreated) LRRK2 silencing induced a significant increase in the number of synaptotagmin and synaptophysin positive clusters (Figure 3C, % of s-tagmin^{+} s-physin^{+} clusters, mean±SE, untreated control=34.17±4.15, siLRRK2=55.87±6.21; n=22, $p<0.01$).

Neurons infected with control virus behaved as non infected neurons while an increase of ratio of recycling synapses was measured when we silenced LRRK2 using miB4 virus (Supplementary Figure 3B-C, % of s-tagmin^{+} s-physin^{+} clusters, mean±SE, non infected=30.90±1.72, control=33.82±1.98, miB4= 55.39±7.89; n=12, $p<0.05$). To test the specificity of the phenotype observed in siLRRK2 neurons, we infected the cells with a virus (miB5) bearing a sequence designed to silence Dlk1, a protein involved in DA neuron differentiation and not expressed at detectable levels in cortical neurons (Bauer et al., 2008). Interestingly, we did not report any increase of the ratio of recycling synapses in miB5 infected neurons (Supplementary Figure 3B-C, % of s-tagmin^{+} s-physin^{+} clusters, mean±SE, miB5=34.59±2.33; n=12, $p>0.05$). We then exposed cultures to anti synaptotagmin Abs in the presence of 50 mM KCl (Figure 3B, KCl). In control neurons the stimulation increased the ratio of recycling synapses as expected (Bacci et al., 2001). However, the siLRRK2 neurons did not react to KCl depolarization (Figure 3C, KCl, % of s-tagmin^{+} s-physin^{+} clusters, mean±SE, control= 79.15±3.22, siLRRK2=60.68±5.47; n=22, $p<0.01$). Finally, once we blocked action potential propagation with 2 μm TTX treatment (Figure 3B, TTX), the ratio of recycling synapses was impaired in both control and siLRRK2 neurons (Figure 3C, TTX, % of s-tagmin^{+} s-physin^{+} clusters, mean±SE, control=21.67±4.16, siLRRK2=27.39±5.63; n=16, $p>0.05$). The total number of synaptic contacts, however, remained unaltered despite pharmacological treatment and viral transduction (Figure 3D and Supplementary Figure 3D, number of s-physin^{+} clusters/10 μm, mean±SE, n=15, $p>0.05$). The observation that LRRK2 silencing increases EPSC and the ratio of recycling synapses might imply that LRRK2 alters the Ca^{2+} affinity of release. To test this hypothesis, we measured the ratio of recycling synapses in the

presence of different concentration of extracellular Ca^{2+} (Yamasaki et al., 2006; Chang and Sudhof, 2009) (Figure 4A). We noticed that overall, siLRRK2 neurons, when compared to control cells, were characterized by a higher ratio of recycling synapses, except when 10 mM extracellular Ca^{2+} concentration was applied (Figure 4B, % of s-tagmin^{+} s-physin^{+} clusters, mean±SE, 0mM Ca^{2+} control= 11.63±1.23, siLRRK2= 16.35±2.87; 2mM Ca^{2+} control=27.02±1.67, siLRRK2=45.70±3.32; 5mM Ca^{2+} control= 42.15±6.36, siLRRK2=60.26±4.27; 10mM Ca^{2+} control=62.09±4.94, siLRRK2= 63.63±5.19 n=14, $p<0.05$). The total number of synaptic contacts, however, remained unaltered (Figure 4C, number of s-physin^{+} clusters/10 μm, mean±SE, n=14, $p>0.05$). These data might indicate that LRRK2 deletion partially alters the Ca^{2+} affinity of release. Another alternative explanation for this phenotype might come from a direct role of LRRK2 in controlling SV trafficking mechanisms. To further test this hypothesis, we analyzed vesicle movement over time. Control, siLRRK2 and miB5 (data not shown) infected neurons were loaded with anti synaptotagmin Abs coupled to Cy3-fluorochrome. Synaptotagmin positive clusters within GFP positive processes were then tracked in basal conditions under laser assisted confocal microscopy (Figure 5A). siRNA mediated LRRK2 knock down increased clusters relative mobility, as demonstrated by analysis of cluster motion over time (Figure 5B shows representative cluster path; see also Supplementary movies 1-8). To compare cluster motion in control, miB5 and siLRRK2 infected cultures, we calculated the diffusion coefficient D from the equation $MSD(\Delta t)= 4D\Delta t$ where $MSD(\Delta t)$ indicate the mean square displacement of the cluster (Saxton, 1982; Kusumi et al., 1993). The coefficient D increased by a Log factor in siLRRK2 neurons when compared to control and miB5 infected neurons (Figure 5C, D [$\mu m^2/s$],

mean±SE, control=0.009±0.0006, miB5=0.011±0.001, siLRRK2=0.152±0.0146; n=9, $p<0.001$). Taken together, these results suggest that LRRK2 modulates vesicle motility inside the presynaptic bouton.

LRRK2 interacts with presynaptic proteins

Since synaptic vesicle mobility and distribution is orchestrated by an array of presynaptic proteins (Sudhof, 2004; Montecucco et al., 2005; Jahn and Scheller, 2006), we tested first if LRRK2 silencing affects synaptic protein expression in cortical neurons. However, we found that the expression of major presynaptic proteins such as NSF, syntaxin 1A, synaptotagmin 1 and synaptophysin as well as actin was not altered by LRRK2 silencing. Also the levels of postsynaptic proteins like PSD-95 and GluR2 were not changed (Supplementary Figure 1B). The function of these proteins is, however, largely conferred via specific protein interactions (Rizo and Rosenmund, 2008; Sudhof and Rothman, 2009). We therefore asked whether LRRK2 in cortical neurons specifically interacts with presynaptic proteins testing for NSF, a vesicle-fusing ATPase and a key player in vesicular endocytosis (Otto et al., 1997; Littleton et al., 1998; Littleton et al., 2001; Kawasaki and Ordway, 2009). NSF was specifically co-precipitated together with endogenous LRRK2 from adult mouse brain lysate using anti LRRK2 1E11 monoclonal antibody (Figure 6A, upper panel). To further prove this finding, we performed a reciprocal immunoprecipitation using a rabbit anti NSF antibody (Figure 6A, lower panel). In fact, NSF co-precipitated endogenous LRRK2 as well as syntaxin1A, a well known interactor of NSF (Hanson et al., 1995). To identify additional LRRK2 interactors from adult mouse brain lysate in a domain specific fashion, we expressed five different

proteins containing specific domains of LRRK2 as GST fusion proteins: GST-N-term, GST-ANK, GST-LRR, GST-Roc-COR-Kinase (GST-R-C-K) and GST-WD40 (Supplementary figure 1C). Pulled proteins were eluted, tryptically digested and the resulting peptides identified by LC-MS/MS (Table 1). The analysis revealed 13 putative interactors specifically binding to GST-LRRK2 domains but not to GST alone. Notably, the interactors found were mainly proteins involved in presynaptic vesicular trafficking, including AP-2 complex subunits, synapsin 1, synaptic vesicle glycoprotein 2A and, as expected, NSF. In order to confirm the results obtained by mass spectrometry all pull-downs were tested by western blotting (Fig 6B). Western blotting confirmed LRRK2 interaction with NSF, syntaxin 1A and actin mainly through its WD40 domain. Furthermore, SNAP-25 and synaptophysin were not found to bind GST-LRRK2 domains (Supplementary Figure 1D). Precedent studies showed LRRK2 is mainly associated with mitochondria but also with multiple vesicles structure, including synaptic vesicles (Biskup et al., 2006). In order to verify if LRRK2 might localize within the cell in a cellular compartment where also its putative interactors are present, we performed a subcellular fractionation of dissociated neuronal cortical cultures (Dodd et al., 1981). LRRK2 showed a partial enrichment in a fraction containing its putative interactors, NSF, syntaxin1A and actin (Figure 6C). Interestingly, also the presynaptic markers Vamp 1, synaptotagmin and the postsynaptic marker PSD-95, but not the cytosolic marker HSP-90, were found enriched in the same fraction (Figure 6D).These data suggest that LRRK2 interacts with a subset of the vesicle fusion protein complex putting it perfectly in place to modulate presynaptic vesicle trafficking and distribution.

LRRK2 silencing alters synaptic vesicle distribution

Synaptic vesicles within the presynaptic compartment are distributed in pools distinguished by the relative distance to the presynaptic membrane (Schikorski and Stevens, 2001; Rizzoli and Betz, 2004). Given the data reported above, we asked if SV number, distribution and clustering might be influenced by LRRK2 silencing. To test this, we analyzed the presynaptic boutons in control and siLRRK2 infected neurons by electron microscopy (Figure 7A). Electron microscopic analysis revealed that LRRK2 knock down did not cause obvious abnormalities in presynaptic terminals with respect to control neurons. LRRK2 silencing did not affect total pool size, as the average number of SV per presynaptic terminal was equal in both conditions (Supplementary figure 4A). Also the analysis of SV dimension, reported by the measurement of major axis length, did not show any differences between the two groups (Supplementary figure 4B). To clarify if LRRK2 might influence synaptic vesicle organization, we analyzed SV distribution in terms of shortest distance to the active zone (AZD) (Nikonenko and Skibo, 2004). We observed differences in the spatial distribution of SV in terms of relative abundance of vesicles located in two specific SV pools, identified by their AZD (Supplementary Figure 4D). siLRRK2 synapses were characterized by a significant reduction in the number of docked SV, i.e. vesicles in physical contact with the presynaptic membrane (Schikorski and Stevens, 2001) (Figure 7C untreated, docked SV [vesicle/μm], mean±SE: control=17±1.32, siLRRK2=11.29±0.53, n=35, $p<0.01$). LRRK2 silencing also caused a significant increase of vesicles located distally to the presynaptic membrane (Figure 7D untreated, fraction of vesicles within a range of 75-150 nm to the presynaptic membrane [%], mean±SE; control=21.11±1.76, siLRRK2=

26.45±1.58, n=35, $p<0.05$). We then depolarized cortical neurons with 50mM KCl before fixation (Figure 7B). LRRK2 silencing did not affect total pool size (Supplementary figure 4C) but altered SV distribution (Supplementary figure 4E). In LRRK2 silenced synapses the amount of docked vesicles was unaltered compared to controls (Figure 7C KCl, docked SV [vesicle/µm], mean±SE: control=10.74±0.51, siLRRK2=10.92±0.48, n=35, $p>0.5$), however, in these neurons the pool within the 75-150nm range was reduced (Figure 7D KCl, fraction of vesicles within a range of 75-150 nm to the presynaptic membrane [%], mean±SE; control=25.28±1.74, siLRRK2=18.88±1.56, n=35, $p<0.01$). To determine if LRRK2 silencing might affect the size of the ready releasable pool (RRP), we applied a hypertonic sucrose pulse (0.5M sucrose, 45s) to cultured neurons while performing the exo-endocytic assay (Figure 8A). Hypertonic sucrose is thought to stimulate the release of the entire RRP in neuron in culture, thereby allowing the estimation of the RRP itself (Rosenmund and Stevens, 1997; Chang and Sudhof, 2009). The hypertonic pulse improved the ratio of recycling synapses in control neurons as expected (Pyle et al., 2000); instead we did not observe any further increase in the ratio of recycling synapses in siLRRK2 neurons. Interestingly control and siLRRK2 neurons demonstrated to uptake synaptotagmin antibody in a similar extent after stimulation (Figure 8B, % of s-tagmin$^+$ s-physin$^+$ clusters, mean±SE: control untreated= 13.58±2.07, 0.5M sucrose= 27.84±1.91; n=15, $p<0.01$; siLRRK2 untreated=24.85±1.66, 0.5M sucrose=26.18±1.51; n=15, $p>0.05$). The total number of synaptic contacts remained unaltered despite the treatments (Figure 8C number of s-physin$^+$ clusters/10 µm, mean±SE, n=15, $p>0.05$). Taken together, these findings suggest an involvement of

LRRK2 in controlling synaptic vesicle distribution within the presynaptic bouton without affecting RRP size.

Discussion

In light of the presented data, we suggest that LRRK2 is part of a functional protein network that controls synaptic vesicle (SV) trafficking within the recycling pool by interacting with a subset of presynaptic proteins. A role of LRRK2 in vesicle trafficking involving Rab5b had already been suggested (Shin et al., 2008) however we can now show for the first time that electrophysiological properties as well as vesicular trafficking in the presynaptic pool depend on the presence of LRRK2 as an integral part of presynaptic protein complex. We have in fact identified presynaptic proteins – NSF, AP-2 complex subunits, SV2A, synapsin and syntaxin 1- as well as actin as putative LRRK2 interactors. These proteins have been previously described as key elements of synaptic vesicle trafficking (Takamori et al., 2006). NSF catalyzes the release of the SNARE complex (SNAP 25, syntaxin 1 and VAMP) and allows the first step of the endocytic cycle (Littleton et al., 1998; Littleton et al., 2001). The clathrin complex [clathrin, AP-2 adaptor complex and accessories protein as dynamin and AP180 (Jung and Haucke, 2007)] constitutes one of the major pathways for SV recycling from the membrane to the resting pool (RP) (Murthy and De Camilli, 2003; Granseth et al., 2006). The control of storage and mobilization of SV in the RRP depends instead on the synaptic vesicle glycoproteins SV2A and B (Xu and Bajjalieh, 2001; Chang and Sudhof, 2009) while synapsins are thought to immobilize SV in the RP by cross-linking vesicles to the actin cytoskeleton (Greengard et al., 1993; Hilfiker et al., 1999). RRP and RP constitute

together the recycling pool [for a more comprehensive review, see (Sudhof, 2000, 2004)]. Ultra-structural analysis of presynaptic boutons revealed that LRRK2 silencing affected the size of a distal pool of SV and the number of docked ones. According to the distance from the active zone, SV within a range of 75-150nm can be considered as belonging to the recycling pool (Schikorski and Stevens, 2001; Genoud et al., 2004). These data suggest LRRK2 is implicated in the mobilization of the recycling pool. The fact that in siLRRK2 neurons synapses we described a similar amount of total SV but a decrease number of docked ones seems to contradict the synaptotagmin uptake and electrophysiology results. But, even if it has generally been assumed that the vesicles closest to release sites and the docked ones represent the RRP and thus are recruited first during synapse activity (Schikorski and Stevens, 2001), studies have shown that the RRP vesicles are distributed without a specific localization within the bouton in a range of 100nm from the active zone (Rizzoli and Betz, 2004). Furthermore, other studies have described modifications of synaptic activity not correlated to ultra-structural changes (Augustin et al., 1999; Rosenmund et al., 2002; Moulder et al., 2006). Other mechanism than docking, such as SV recruiting, priming or release efficacy, might be involved in synaptic adaptation to activity (Morales et al., 2000; Moulder et al., 2006). Given that we did not discriminate between resting SV and recycling SV in our ultra-structural analysis, we cannot draw here a direct link between distribution/number of vesicle and fusion events. Notwithstanding this, in our hands, control neurons exhibited a reduction of docked vesicle after KCl depolarization, effect that might be related to massive vesicle release. Similarly, we described here a reduced amount of docked SV in basal condition after LRRK2 knock down. This outcome might arise or from a reduction of RRP size or

from an alteration of firing rate or/and vesicle fusion probability. Given that the total RRP size, as estimated by hypertonic sucrose application, was not altered in siLRRK2 neurons, we propose that the lack of LRRK2 affects SV release. Accordingly, the ratio of recycling synapses, monitored by anti synaptotagmin antibody uptake, was increased in siLRRK2 neurons under basal conditions. Interestingly, we observed in siLRRK2 silenced neurons an inability to further increase the ratio of recycling synapses after long lasting depolarization. This lack of response may reflect the depletion of the RRP due to a perturbation of the recycling machinery. In fact, it has been shown that sustained repetitive activity beyond the first presynaptic release depends not only on the RRP but on SV mobilization from the RP to overcome the rapid depletion of RRP (Dobrunz and Stevens, 1997; Murthy and Stevens, 1998). Indeed, the distribution of SV after long lasting depolarization was altered by LRRK2 silencing. Given that the blockage of action potential propagation through TTX treatment impaired the ratio of recycling synapses in both control and siLRRK2 neurons, we suggest that LRRK2 participates mainly in the trafficking of SV driven by evoked activity. Our findings that the presynaptic lack of LRRK2 alters excitatory postsynaptic current (EPSC) further support the idea of an involvement of LRRK2 in presynaptic mechanisms. EPSC amplitude depends on the presynaptic factors of vesicle number (N), probability of successful fusion (P) together with the postsynaptic quantal response (Q), EPSC=NPQ [reviewed in (Schneggenburger et al., 2002)]. Indeed, LRRK2 silencing in the presynaptic neurons was associated with a reduction in failure rate and with an increase of EPSC amplitude following a single stimulation. Furthermore LRRK2 silencing induced a significant paired pulse depression and an increase of the second current latency. In a simple model, PPD can be explained

as the consequence of the depletion of RRP after multiple triggers (Zucker and Regehr, 2002), but experimental evidences have enlightened how other mechanisms might influence short term plasticity (Waldeck et al., 2000; Xu and Wu, 2005; Sullivan, 2007). PPD has been associated to an increased latency and a reduction of P (Waldeck et al., 2000; Boudkkazi et al., 2007); additionally, manipulation that modifies P significantly affects synaptic latency (Boudkkazi et al., 2007). Variations in P might derive from local modifications of presynaptic Ca^{2+} concentrations, from modulation of the Ca^{2+} sensitivity of the release machinery and finally from the availability and the correct spatial organization of the components of the fusion machinery (Matz et al.; Paisan-Ruiz et al., 2004; Wadel et al., 2007; Kawasaki and Ordway, 2009). The analysis of the ratio of recycling synapses at different Ca^{2+} concentrations might suggest that LRRK2 silencing affects Ca^{2+} sensitivity. Another explanation for the effect on evoked currents we registered during single or repetitive stimulation might arise from a disorganization of SV storage and/or mobilization. FRAP measurements of SV mobility have concluded that recycling vesicles have poor mobility in cultured hippocampal neurons (D~0.003 $\mu m^2/s$) (Gaffield et al., 2006). This tight confinement depends on molecular anchors such as synapsins and actin and is functional to a correct SV trafficking [for a comprehensive review, see (Rizzoli and Betz, 2005)]. But interestingly, neither synapsins KO nor actin filament disruption has been shown to increase severely SV mobility (Gaffield et al., 2006; Gaffield and Betz, 2007). Thus, synapsins and actin are not uniquely required for the regulation of SV dynamics but they might act in cooperation with other molecules. We propose that LRRK2 executes its main function at the presynaptic site; given its relative position as an integral part of a presynaptic protein network, LRRK2 may serve

as a molecular hub coordinating both the storage and the mobilization of SV driven by activity. Accordingly, the analysis of vesicle motion showed that SV in siLRRK2 neurons were characterized by an increased spatial freedom, with a measured diffusion coefficient approaching that of vesicles in free solution (D~0.15 $\mu m^2/s$) (Luby-Phelps et al., 1987). Therefore, if in basal condition the lack of LRRK2 might confer to vesicles a higher probability to contact the membrane and fuse, it might as well affect the organization of the presynaptic machinery thus impairing SV mobilization required during high activity. An intriguing possibility yet to be explored is that the impact of LRRK2 on SV trafficking mainly interests silent synapses (Moulder et al., 2004; Moulder et al., 2006; Moulder et al., 2008) or the pool of reluctant vesicles described in glutamatergic terminals (Sun and Wu, 2001; Moulder and Mennerick, 2005). In fact, interestingly, LRRK2 knock down and hypertonic sucrose stimulation were associated with a comparable increase in the ratio of recycling synapses. This might suggest that LRRK2 controls a pool of SV larger than the RRP that is not involved during basal activity but instead can be released by hypertonic sucrose stimulation (Moulder and Mennerick, 2005). Even if a recent study (Andres-Mateos et al., 2009) has reported that LRRK2 knockout in mice does not result in any observable phenotype, it has been shown that LRRK2 mutation affects activity-dependent DA neurotransmission and catecholamine release (Tong et al., 2009). Furthermore, considering the complexity and the importance of the fusion machinery and the expression in neurons of a homologous of LRRK2, LRRK1 (Biskup et al., 2007; Westerlund et al., 2008), compensatory mechanisms during embryonic development of LRRK2 knock out mice cannot be excluded. Data obtained from our domain based interaction studies finally suggest that

LRRK2 interacts with presynaptic partners mainly through its WD40 C-terminal domain. This domain is required for both LRRK2 toxic and physiological role (Sheng et al.; Jorgensen et al., 2009) and it harbors the mutation G2385R, considered as the main risk factor for Parkinson' disease in Chinese Han population (Mata et al., 2005). Future studies are now needed to determine whether perturbed regulation of vesicle trafficking may contribute to Parkinson's disease associated with this gene variant. Given the correlation recently described between LRRK2 and α-synuclein (Carballo-Carbajal et al.; Lin et al., 2009) and the impact of α-synuclein over-expression on synaptic vesicle recycling (Nemani et al., 2010), the regulation of neurotransmitter release might arise as one the main biological pathway compromised during neuropathology onset.

References

Aasly JO, Toft M, Fernandez-Mata I, Kachergus J, Hulihan M, White LR, Farrer M (2005) Clinical features of LRRK2-associated Parkinson's disease in central Norway. Ann Neurol 57:762-765.

Andres-Mateos E, Mejias R, Sasaki M, Li X, Lin BM, Biskup S, Zhang L, Banerjee R, Thomas B, Yang L, Liu G, Beal MF, Huso DL, Dawson TM, Dawson VL (2009) Unexpected lack of hypersensitivity in LRRK2 knock-out mice to MPTP (1-methyl-4-phenyl-1,2,3,6-tetrahydropyridine). J Neurosci 29:15846-15850.

Augustin I, Rosenmund C, Sudhof TC, Brose N (1999) Munc13-1 is essential for fusion competence of glutamatergic synaptic vesicles. Nature 400:457-461.

Bacci A, Coco S, Pravettoni E, Schenk U, Armano S, Frassoni C, Verderio C, De Camilli P, Matteoli M (2001) Chronic blockade of glutamate receptors enhances presynaptic release and downregulates the interaction between synaptophysin-synaptobrevin-vesicle-associated membrane protein 2. J Neurosci 21:6588-6596.

Bardoni R, Torsney C, Tong CK, Prandini M, MacDermott AB (2004) Presynaptic NMDA receptors modulate glutamate release from primary sensory neurons in rat spinal cord dorsal horn. J Neurosci 24:2774-2781.

Bauer M, Kinkl N, Meixner A, Kremmer E, Riemenschneider M, Forstl H, Gasser T, Ueffing M (2009) Prevention of interferon-stimulated gene expression using microRNA-designed hairpins. Gene Ther 16:142-147.

Bauer M, Szulc J, Meyer M, Jensen CH, Terki TA, Meixner A, Kinkl N, Gasser T, Aebischer P, Ueffing M (2008) Delta-like 1 participates in the specification of ventral midbrain progenitor derived dopaminergic neurons. J Neurochem 104:1101-1115.

Berg D, Schweitzer K, Leitner P, Zimprich A, Lichtner P, Belcredi P, Brussel T, Schulte C, Maass S, Nagele T (2005) Type and frequency of mutations in the LRRK2 gene in familial and sporadic Parkinson's disease*. Brain 128:3000-3011.

Biskup S, Moore DJ, Rea A, Lorenz-Deperieux B, Coombes CE, Dawson VL, Dawson TM, West AB (2007) Dynamic and redundant regulation of LRRK2 and LRRK1 expression. BMC Neurosci 8:102.

Biskup S, Moore DJ, Celsi F, Higashi S, West AB, Andrabi SA, Kurkinen K, Yu SW, Savitt JM, Waldvogel HJ, Faull RL, Emson PC, Torp R, Ottersen OP, Dawson TM, Dawson VL (2006) Localization of LRRK2 to membranous and vesicular structures in mammalian brain. Ann Neurol 60:557-569.

Bonifati V (2006) Parkinson's disease: the LRRK2-G2019S mutation: opening a novel era in Parkinson's disease genetics. Eur J Hum Genet 14:1061-1062.

Bosgraaf L, Van Haastert PJ (2003) Roc, a Ras/GTPase domain in complex proteins. Biochim Biophys Acta 1643:5-10.

Boudkkazi S, Carlier E, Ankri N, Caillard O, Giraud P, Fronzaroli-Molinieres L, Debanne D (2007) Release-dependent variations in synaptic latency: a putative code for short- and long-term synaptic dynamics. Neuron 56:1048-1060.

Brice A (2005) Genetics of Parkinson's disease: LRRK2 on the rise. Brain 128:2760-2762.

Buckby LE, Mummery R, Crompton MR, Beesley PW, Empson RM (2004) Comparison of neuroplastin and synaptic marker protein expression in acute and cultured organotypic hippocampal slices from rat. Brain Res Dev Brain Res 150:1-7.

Carballo-Carbajal I, Weber-Endress S, Rovelli G, Chan D, Wolozin B, Klein CL, Patenge N, Gasser T, Kahle PJ Leucine-rich repeat kinase 2 induces alpha-synuclein expression via the extracellular signal-regulated kinase pathway. Cell Signal 22:821-827.

Chang WP, Sudhof TC (2009) SV2 renders primed synaptic vesicles competent for Ca2+ -induced exocytosis. J Neurosci 29:883-897.

Dobrunz LE, Stevens CF (1997) Heterogeneity of release probability, facilitation, and depletion at central synapses. Neuron 18:995-1008.

Dodd PR, Hardy JA, Oakley AE, Edwardson JA, Perry EK, Delaunoy JP (1981) A rapid method for preparing synaptosomes: comparison, with alternative procedures. Brain Res 226:107-118.

Eng JK, McCormack AL, Yates JRr (1994) An approach to correlate tandem mass spectral data of peptides with amino acid sequences in a protein database. Journal of the American Society for Mass Spectrometry 5:976-989.

Frangioni JV, Neel BG (1993) Solubilization and purification of enzymatically active glutathione S-transferase (pGEX) fusion proteins. Anal Biochem 210:179-187.

Gaffield MA, Betz WJ (2007) Synaptic vesicle mobility in mouse motor nerve terminals with and without synapsin. J Neurosci 27:13691-13700.

Gaffield MA, Rizzoli SO, Betz WJ (2006) Mobility of synaptic vesicles in different pools in resting and stimulated frog motor nerve terminals. Neuron 51:317-325.

Genoud C, Knott GW, Sakata K, Lu B, Welker E (2004) Altered synapse formation in the adult somatosensory cortex of brain-derived neurotrophic factor heterozygote mice. J Neurosci 24:2394-2400.

Gillardon F (2009) Leucine-rich repeat kinase 2 phosphorylates brain tubulin-beta isoforms and modulates microtubule stability - a point of convergence in Parkinsonian neurodegeneration? J Neurochem.

Gloeckner CJ, Schumacher A, Boldt K, Ueffing M (2009) The Parkinson disease-associated protein kinase LRRK2 exhibits MAPKKK activity and phosphorylates MKK3/6 and MKK4/7, in vitro. J Neurochem 109:959-968.

Gloeckner CJ, Kinkl N, Schumacher A, Braun RJ, O'Neill E, Meitinger T, Kolch W, Prokisch H, Ueffing M (2006) The Parkinson disease causing LRRK2 mutation I2020T is associated with increased kinase activity. Hum Mol Genet 15:223-232.

Goldwurm S et al. (2005) The G6055A (G2019S) mutation in LRRK2 is frequent in both early and late onset Parkinson's disease and originates from a common ancestor. J Med Genet 42:e65.

Granseth B, Odermatt B, Royle SJ, Lagnado L (2006) Clathrin-mediated endocytosis is the dominant mechanism of vesicle retrieval at hippocampal synapses. Neuron 51:773-786.

Greengard P, Valtorta F, Czernik AJ, Benfenati F (1993) Synaptic vesicle phosphoproteins and regulation of synaptic function. Science 259:780-785.

Greggio E, Jain S, Kingsbury A, Bandopadhyay R, Lewis P, Kaganovich A, van der Brug MP, Beilina A, Blackinton J, Thomas KJ, Ahmad R, Miller DW, Kesavapany S, Singleton A, Lees A, Harvey RJ, Harvey K, Cookson MR (2006) Kinase activity

is required for the toxic effects of mutant LRRK2/dardarin. Neurobiol Dis 23:329-341.
Guo L, Wang W, Chen SG (2006) Leucine-rich repeat kinase 2: relevance to Parkinson's disease. Int J Biochem Cell Biol 38:1469-1475.
Hanson PI, Otto H, Barton N, Jahn R (1995) The N-ethylmaleimide-sensitive fusion protein and alpha-SNAP induce a conformational change in syntaxin. J Biol Chem 270:16955-16961.
Hardy J, Cai H, Cookson MR, Gwinn-Hardy K, Singleton A (2006) Genetics of Parkinson's disease and parkinsonism. Ann Neurol 60:389-398.
Higashi S, Moore DJ, Colebrooke RE, Biskup S, Dawson VL, Arai H, Dawson TM, Emson PC (2007) Expression and localization of Parkinson's disease-associated leucine-rich repeat kinase 2 in the mouse brain. J Neurochem 100:368-381.
Hilfiker S, Pieribone VA, Czernik AJ, Kao HT, Augustine GJ, Greengard P (1999) Synapsins as regulators of neurotransmitter release. Philos Trans R Soc Lond B Biol Sci 354:269-279.
Iaccarino C, Crosio C, Vitale C, Sanna G, Carri MT, Barone P (2007) Apoptotic mechanisms in mutant LRRK2-mediated cell death. Hum Mol Genet 16:1319-1326.
Jahn R, Scheller RH (2006) SNAREs--engines for membrane fusion. Nat Rev Mol Cell Biol 7:631-643.
Jorgensen ND, Peng Y, Ho CC, Rideout HJ, Petrey D, Liu P, Dauer WT (2009) The WD40 domain is required for LRRK2 neurotoxicity. PLoS One 4:e8463.
Jung N, Haucke V (2007) Clathrin-mediated endocytosis at synapses. Traffic 8:1129-1136.
Kawasaki F, Ordway RW (2009) Molecular mechanisms determining conserved properties of short-term synaptic depression revealed in NSF and SNAP-25 conditional mutants. Proc Natl Acad Sci U S A 106:14658-14663.
Keller A, Nesvizhskii AI, Kolker E, Aebersold R (2002) Empirical statistical model to estimate the accuracy of peptide identifications made by MS/MS and database search. Anal Chem 74:5383-5392.
Kraszewski K, Mundigl O, Daniell L, Verderio C, Matteoli M, De Camilli P (1995) Synaptic vesicle dynamics in living cultured hippocampal neurons visualized with CY3-conjugated antibodies directed against the lumenal domain of synaptotagmin. J Neurosci 15:4328-4342.
Kusumi A, Sako Y, Yamamoto M (1993) Confined lateral diffusion of membrane receptors as studied by single particle tracking (nanovid microscopy). Effects of calcium-induced differentiation in cultured epithelial cells. Biophys J 65:2021-2040.
Lee SH, Sheng M (2000) Development of neuron-neuron synapses. Curr Opin Neurobiol 10:125-131.
Li X, Moore DJ, Xiong Y, Dawson TM, Dawson VL (2010) Reevaluation of phosphorylation sites in the Parkinson's disease associated leucine rich repeat kinase-2. J Biol Chem.
Lin X, Parisiadou L, Gu XL, Wang L, Shim H, Sun L, Xie C, Long CX, Yang WJ, Ding J, Chen ZZ, Gallant PE, Tao-Cheng JH, Rudow G, Troncoso JC, Liu Z, Li Z, Cai H (2009) Leucine-rich repeat kinase 2 regulates the progression of

neuropathology induced by Parkinson's-disease-related mutant alpha-synuclein. Neuron 64:807-827.
Littleton JT, Chapman ER, Kreber R, Garment MB, Carlson SD, Ganetzky B (1998) Temperature-sensitive paralytic mutations demonstrate that synaptic exocytosis requires SNARE complex assembly and disassembly. Neuron 21:401-413.
Littleton JT, Barnard RJ, Titus SA, Slind J, Chapman ER, Ganetzky B (2001) SNARE-complex disassembly by NSF follows synaptic-vesicle fusion. Proc Natl Acad Sci U S A 98:12233-12238.
Luby-Phelps K, Castle PE, Taylor DL, Lanni F (1987) Hindered diffusion of inert tracer particles in the cytoplasm of mouse 3T3 cells. Proc Natl Acad Sci U S A 84:4910-4913.
MacLeod D, Dowman J, Hammond R, Leete T, Inoue K, Abeliovich A (2006) The familial Parkinsonism gene LRRK2 regulates neurite process morphology. Neuron 52:587-593.
Malgaroli A, Ting AE, Wendland B, Bergamaschi A, Villa A, Tsien RW, Scheller RH (1995) Presynaptic component of long-term potentiation visualized at individual hippocampal synapses. Science 268:1624-1628.
Markram H, Lubke J, Frotscher M, Roth A, Sakmann B (1997) Physiology and anatomy of synaptic connections between thick tufted pyramidal neurones in the developing rat neocortex. J Physiol 500 (Pt 2):409-440.
Mata IF, Kachergus JM, Taylor JP, Lincoln S, Aasly J, Lynch T, Hulihan MM, Cobb SA, Wu RM, Lu CS, Lahoz C, Wszolek ZK, Farrer MJ (2005) Lrrk2 pathogenic substitutions in Parkinson's disease. Neurogenetics 6:171-177.
Matteoli M, Takei K, Perin MS, Sudhof TC, De Camilli P (1992) Exo-endocytotic recycling of synaptic vesicles in developing processes of cultured hippocampal neurons. J Cell Biol 117:849-861.
Matveev V, Sherman A, Zucker RS (2002) New and corrected simulations of synaptic facilitation. Biophys J 83:1368-1373.
Matz J, Gilyan A, Kolar A, McCarvill T, Krueger SR Rapid structural alterations of the active zone lead to sustained changes in neurotransmitter release. Proc Natl Acad Sci U S A 107:8836-8841.
Melrose H, Lincoln S, Tyndall G, Dickson D, Farrer M (2006) Anatomical localization of leucine-rich repeat kinase 2 in mouse brain. Neuroscience 139:791-794.
Mielke JG, Comas T, Woulfe J, Monette R, Chakravarthy B, Mealing GA (2005) Cytoskeletal, synaptic, and nuclear protein changes associated with rat interface organotypic hippocampal slice culture development. Brain Res Dev Brain Res 160:275-286.
Montecucco C, Schiavo G, Pantano S (2005) SNARE complexes and neuroexocytosis: how many, how close? Trends Biochem Sci 30:367-372.
Moore DJ, West AB, Dawson VL, Dawson TM (2005) Molecular pathophysiology of Parkinson's disease. Annu Rev Neurosci 28:57-87.
Morales M, Colicos MA, Goda Y (2000) Actin-dependent regulation of neurotransmitter release at central synapses. Neuron 27:539-550.
Moulder KL, Mennerick S (2005) Reluctant vesicles contribute to the total readily releasable pool in glutamatergic hippocampal neurons. J Neurosci 25:3842-3850.

Moulder KL, Jiang X, Taylor AA, Olney JW, Mennerick S (2006) Physiological activity depresses synaptic function through an effect on vesicle priming. J Neurosci 26:6618-6626.
Moulder KL, Meeks JP, Shute AA, Hamilton CK, de Erausquin G, Mennerick S (2004) Plastic elimination of functional glutamate release sites by depolarization. Neuron 42:423-435.
Moulder KL, Jiang X, Chang C, Taylor AA, Benz AM, Conti AC, Muglia LJ, Mennerick S (2008) A specific role for Ca2+-dependent adenylyl cyclases in recovery from adaptive presynaptic silencing. J Neurosci 28:5159-5168.
Murthy VN, Stevens CF (1998) Synaptic vesicles retain their identity through the endocytic cycle. Nature 392:497-501.
Murthy VN, De Camilli P (2003) Cell biology of the presynaptic terminal. Annu Rev Neurosci 26:701-728.
Nemani VM, Lu W, Berge V, Nakamura K, Onoa B, Lee MK, Chaudhry FA, Nicoll RA, Edwards RH (2010) Increased expression of alpha-synuclein reduces neurotransmitter release by inhibiting synaptic vesicle reclustering after endocytosis. Neuron 65:66-79.
Nesvizhskii AI, Aebersold R (2004) Analysis, statistical validation and dissemination of large-scale proteomics datasets generated by tandem MS. Drug Discov Today 9:173-181.
Nikonenko AG, Skibo GG (2004) Technique to quantify local clustering of synaptic vesicles using single section data. Microsc Res Tech 65:287-291.
Olsen JV, de Godoy LM, Li G, Macek B, Mortensen P, Pesch R, Makarov A, Lange O, Horning S, Mann M (2005) Parts per million mass accuracy on an Orbitrap mass spectrometer via lock mass injection into a C-trap. Mol Cell Proteomics 4:2010-2021.
Otto H, Hanson PI, Jahn R (1997) Assembly and disassembly of a ternary complex of synaptobrevin, syntaxin, and SNAP-25 in the membrane of synaptic vesicles. Proc Natl Acad Sci U S A 94:6197-6201.
Paisan-Ruiz C et al. (2004) Cloning of the gene containing mutations that cause PARK8-linked Parkinson's disease. Neuron 44:595-600.
Plowey ED, Cherra SJ, 3rd, Liu YJ, Chu CT (2008) Role of autophagy in G2019S-LRRK2-associated neurite shortening in differentiated SH-SY5Y cells. J Neurochem 105:1048-1056.
Pyle JL, Kavalali ET, Piedras-Renteria ES, Tsien RW (2000) Rapid reuse of readily releasable pool vesicles at hippocampal synapses. Neuron 28:221-231.
Rizo J, Rosenmund C (2008) Synaptic vesicle fusion. Nat Struct Mol Biol 15:665-674.
Rizzoli SO, Betz WJ (2004) The structural organization of the readily releasable pool of synaptic vesicles. Science 303:2037-2039.
Rizzoli SO, Betz WJ (2005) Synaptic vesicle pools. Nat Rev Neurosci 6:57-69.
Romorini S, Piccoli G, Jiang M, Grossano P, Tonna N, Passafaro M, Zhang M, Sala C (2004) A functional role of postsynaptic density-95-guanylate kinase-associated protein complex in regulating Shank assembly and stability to synapses. J Neurosci 24:9391-9404.
Rosenmund C, Stevens CF (1997) The rate of aldehyde fixation of the exocytotic machinery in cultured hippocampal synapses. J Neurosci Methods 76:1-5.

Rosenmund C, Sigler A, Augustin I, Reim K, Brose N, Rhee JS (2002) Differential control of vesicle priming and short-term plasticity by Munc13 isoforms. Neuron 33:411-424.

Rudelius M, Osanger A, Kohlmann S, Augustin M, Piontek G, Heinzmann U, Jennen G, Russ A, Matiasek K, Stumm G, Schlegel J (2006) A missense mutation in the WD40 domain of murine Lyst is linked to severe progressive Purkinje cell degeneration. Acta Neuropathol 112:267-276.

Saxton MJ (1982) Lateral diffusion in an archipelago. Effects of impermeable patches on diffusion in a cell membrane. Biophys J 39:165-173.

Saxton MJ (1994) Single-particle tracking: models of directed transport. Biophys J 67:2110-2119.

Sbalzarini IF, Koumoutsakos P (2005) Feature point tracking and trajectory analysis for video imaging in cell biology. J Struct Biol 151:182-195.

Schikorski T, Stevens CF (2001) Morphological correlates of functionally defined synaptic vesicle populations. Nat Neurosci 4:391-395.

Schneggenburger R, Sakaba T, Neher E (2002) Vesicle pools and short-term synaptic depression: lessons from a large synapse. Trends Neurosci 25:206-212.

Sheng D, Qu D, Kwok KH, Ng SS, Lim AY, Aw SS, Lee CW, Sung WK, Tan EK, Lufkin T, Jesuthasan S, Sinnakaruppan M, Liu J Deletion of the WD40 domain of LRRK2 in Zebrafish causes Parkinsonism-like loss of neurons and locomotive defect. PLoS Genet 6:e1000914.

Shin N, Jeong H, Kwon J, Heo HY, Kwon JJ, Yun HJ, Kim CH, Han BS, Tong Y, Shen J, Hatano T, Hattori N, Kim KS, Chang S, Seol W (2008) LRRK2 regulates synaptic vesicle endocytosis. Exp Cell Res 314:2055-2065.

Sudhof TC (2000) The synaptic vesicle cycle revisited. Neuron 28:317-320.

Sudhof TC (2004) The synaptic vesicle cycle. Annu Rev Neurosci 27:509-547.

Sudhof TC, Rothman JE (2009) Membrane fusion: grappling with SNARE and SM proteins. Science 323:474-477.

Sullivan JM (2007) A simple depletion model of the readily releasable pool of synaptic vesicles cannot account for paired-pulse depression. J Neurophysiol 97:948-950.

Sun JY, Wu LG (2001) Fast kinetics of exocytosis revealed by simultaneous measurements of presynaptic capacitance and postsynaptic currents at a central synapse. Neuron 30:171-182.

Takamori S et al. (2006) Molecular anatomy of a trafficking organelle. Cell 127:831-846.

Taylor JP, Mata IF, Farrer MJ (2006) LRRK2: a common pathway for parkinsonism, pathogenesis and prevention? Trends Mol Med 12:76-82.

Tong Y, Pisani A, Martella G, Karouani M, Yamaguchi H, Pothos EN, Shen J (2009) R1441C mutation in LRRK2 impairs dopaminergic neurotransmission in mice. Proc Natl Acad Sci U S A.

Verderio C, Coco S, Bacci A, Rossetto O, De Camilli P, Montecucco C, Matteoli M (1999) Tetanus toxin blocks the exocytosis of synaptic vesicles clustered at synapses but not of synaptic vesicles in isolated axons. J Neurosci 19:6723-6732.

Wadel K, Neher E, Sakaba T (2007) The coupling between synaptic vesicles and Ca2+ channels determines fast neurotransmitter release. Neuron 53:563-575.

Waldeck RF, Pereda A, Faber DS (2000) Properties and plasticity of paired-pulse depression at a central synapse. J Neurosci 20:5312-5320.

Wang L, Xie C, Greggio E, Parisiadou L, Shim H, Sun L, Chandran J, Lin X, Lai C, Yang WJ, Moore DJ, Dawson TM, Dawson VL, Chiosis G, Cookson MR, Cai H (2008) The chaperone activity of heat shock protein 90 is critical for maintaining the stability of leucine-rich repeat kinase 2. J Neurosci 28:3384-3391.

West AB, Moore DJ, Biskup S, Bugayenko A, Smith WW, Ross CA, Dawson VL, Dawson TM (2005) Parkinson's disease-associated mutations in leucine-rich repeat kinase 2 augment kinase activity. Proc Natl Acad Sci U S A 102:16842-16847.

Westerlund M, Belin AC, Anvret A, Bickford P, Olson L, Galter D (2008) Developmental regulation of leucine-rich repeat kinase 1 and 2 expression in the brain and other rodent and human organs: Implications for Parkinson's disease. Neuroscience 152:429-436.

Wiznerowicz M, Trono D (2003) Conditional suppression of cellular genes: lentivirus vector-mediated drug-inducible RNA interference. J Virol 77:8957-8961.

Xu J, Wu LG (2005) The decrease in the presynaptic calcium current is a major cause of short-term depression at a calyx-type synapse. Neuron 46:633-645.

Xu T, Bajjalieh SM (2001) SV2 modulates the size of the readily releasable pool of secretory vesicles. Nat Cell Biol 3:691-698.

Yamasaki M, Hashimoto K, Kano M (2006) Miniature synaptic events elicited by presynaptic Ca2+ rise are selectively suppressed by cannabinoid receptor activation in cerebellar Purkinje cells. J Neurosci 26:86-95.

Zimprich A et al. (2004) The PARK8 locus in autosomal dominant parkinsonism: confirmation of linkage and further delineation of the disease-containing interval. Am J Hum Genet 74:11-19.

Ziv NE, Garner CC (2001) Principles of glutamatergic synapse formation: seeing the forest for the trees. Curr Opin Neurobiol 11:536-543.

Zucker RS, Regehr WG (2002) Short-term synaptic plasticity. Annu Rev Physiol 64:355-405.

Figure legends

Figure 1. LRRK2 expression increases during in vitro neuron development. (A) Neurons were cultured and solubilized at the indicated DIV. Equal amounts of protein were loaded on SDS-PAGE gel and stained with the indicated antibodies. LRRK2 expression increases along in vitro synapse maturation, as demonstrated by the parallel increment of PSD-95 and synaptophysin amount. Two representative independent experiments are shown. (B) Mean protein levels (±SE) expressed as optical density (in arbitrary unit) normalized against total protein amount; n=5, * $p<0.05$ versus DIV4. (C) Cortical neurons were left untreated (mock) or infected at DIV10 with control (LVTH) or two LRRK2 silencing (miB3 and miB4) viruses, solubilized at DIV18 and analyzed for the expression of the indicated protein. (D) LRRK2 protein levels expressed as percentage over control, mean±SE; **$p<0.01$, n=5, ANOVA followed by Tukey's post hoc test

Figure 2. LRRK2 silencing modifies synaptic transmission. Paired recordings were performed between a control or siLRRK2 transfected neuron (presynaptic) and an adjacent non-transfected neuron. (A) Representative EPSC traces from control and siLRRK2 pairs after a single depolarizing stimulus (100mV, 1ms). (B) Representative traces from control and siLRRK2 pairs after a paired pulse stimulation protocol (100 mV, 1ms, 50 ms inter pulse interval). (C) LRRK2 silencing significantly increased evoked EPSC amplitude after a single pulse stimulation while enhances paired pulse depression. (D) LRRK2 silencing increased the latency of the second EPSC. Data are expressed as mean±SE, ** $p<0.01$, *** $p<0.001$, Student's T-test, n=5.

Figure 3. LRRK2 silencing modifies synaptic vesicle recycling. The synaptotagmin uptake assay was performed on cortical neurons at DIV18, infected at DIV10 with control or siLRRK2 virus. (A) Synaptotagmin (s-tagmin) positive spots co-localized with synaptophysin (s-physin) clusters along neuron processes. (B) Neurons were left untreated or treated with KCl (50 mM 5 minutes) or TTX (30 minutes before labelling, 2 μM) and then assayed for exo-endo cytosis. Scale bar = 5 μm. (C) The percentage of s-tagmin and s-physin positive clusters within the totality of s-physin positive clusters reflects the pool of recycling synapses. LRRK2 silenced neurons showed an increased ratio of recycling synapses in basal condition, but a reduced activity after KCl stimulation. Instead LRRK2 knock down did not modify the number of recycling synapses during TTX repression. (D) Active zone number, monitored as synaptophysin positive dots along neuronal processes, was not modified by LRRK2 silencing. Data are expressed as mean±SE; * $p<0.05$, ** $p<0.01$, same treatment, Student T-test, # $p<0.01$ same infection, ANOVA, Tukey's post hoc test, n=25.

Figure 4. LRRK2 silencing affects Ca^{2+} sensitivity. (A) The ratio of recycling synapses was assayed in neurons in presence of increasing external Ca^{2+} concentration. Scale bar = 5 μm. (B) The ratio of recycling synapses rose to a higher extent in siLRRK2 neurons in response to increasing Ca^{2+} concentration. (C) Active zone number was not modified by LRRK2 silencing or Ca^{2+} concentration. Data are expressed as mean±SE; * $p<0.05$ vs control Student´s T-test, n=14.

Figure 5. LRRK2 silencing increases vesicle motility. (A) Control and siLRRK2 infected neurons were exposed to anti synaptotagmin antibody coupled to a fluorochrome. Synaptotagmin positive clusters within GFP positive processes were tracked in basal condition under laser confocal microscopy. Clusters in siLRRK2 neurons showed an increased motility. Yellow arrows indicate the position of cluster at t=0 s. White arrows report instead the position of the clusters relative to the previous time point. Scale bar= 5 μm. (B) The diagram reports representative path of single cluster from control or siLRRK2 neuron. Scale bar=1μm. (C) Quantification of diffusion coefficient D, where MSD(Δt)=4Dt; mean ±SE; ***p<0.001, Student's T-test, n=9.

Figure 6 LRRK2 interacts with presynaptic protein. (A) Immunoprecipitation of endogenous LRRK2 (upper panel) and NSF (lower panel) from adult brain lysate shows that LRRK2 and NSF interact physiologically. NSF antibody precipitates equally syntaxin1 and LRRK2. (B) LRRK2 interacts with presynaptic proteins. GST-LRRK2 domains have been used to pull-down putative LRRK2 interactors from adult mouse brain. LRRK2 WD40 domain precipitates presynaptic proteins as NSF and syntaxin 1A and actin. (C-D) LRRK2 is present in a sub-cellular fraction (P3) where its putative interactors and pre and postsynaptic markers are found. s-tagmin=synaptotagmin.

Figure 7. LRRK2 silencing perturbs vesicle distribution inside the presynaptic bouton. Neurons were infected at DIV10 as described and processed for electron-microscopy at DIV18. (A-B) High magnification (40,000X) images from control or LRRK2 silenced neurons kept in basal condition (A) or depolarized with 50mM KCl 5 minutes (B). (C)

The number of docked vesicle (vesicle/μm presynaptic membrane) was reduced in siLRRK2 neurons kept in basal condition. (D) LRRK2 silencing affected the fraction of total vesicle within 75-150nm range from the presynaptic membrane in untreated and depolarized neurons. Data are expressed as mean±SE, *p<0.05, **p<0.01 Student-T test, n=35. Scale bar = 500 nm.

Figure 8. LRRK2 silencing does not affect RRP size. (A) The ratio of recycling synapses was assayed in neurons in presence of a hypertonic sucrose solution (0.5M sucrose, 45s). Scale bar = 5 μm. (B) The ratio of recycling synapses was not significantly different between control and siLRRK2 neurons after sucrose application. Data are expressed as mean±SE; * p<0.05 vs control # p<0.05 vs untreated, ANOVA, Tukey's post hoc test, n=15.

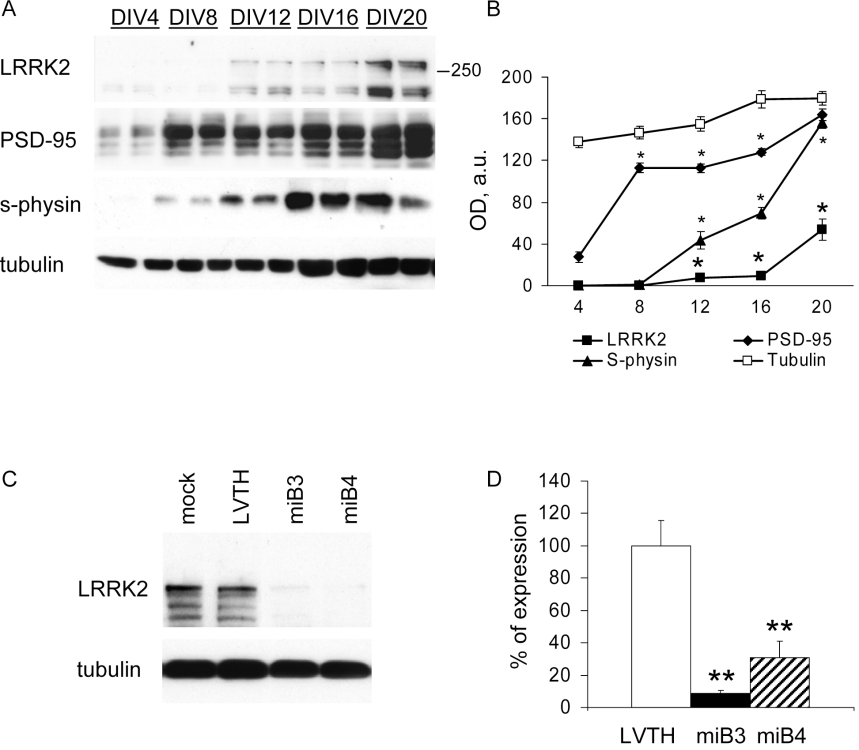
A
DIV4 DIV8 DIV12 DIV16 DIV20
LRRK2
PSD-95
s-physin
tubulin
250
B
OD, a.u.
200
160
120
80
40
0
4
8
12
16
20
LRRK2
PSD-95
S-physin
Tubulin
C
mock
LVTH
miB3
miB4
LRRK2
tubulin
D
% of expression
140
120
100
80
60
40
20
0
**
**
LVTH
miB3
miB4

Figure 1

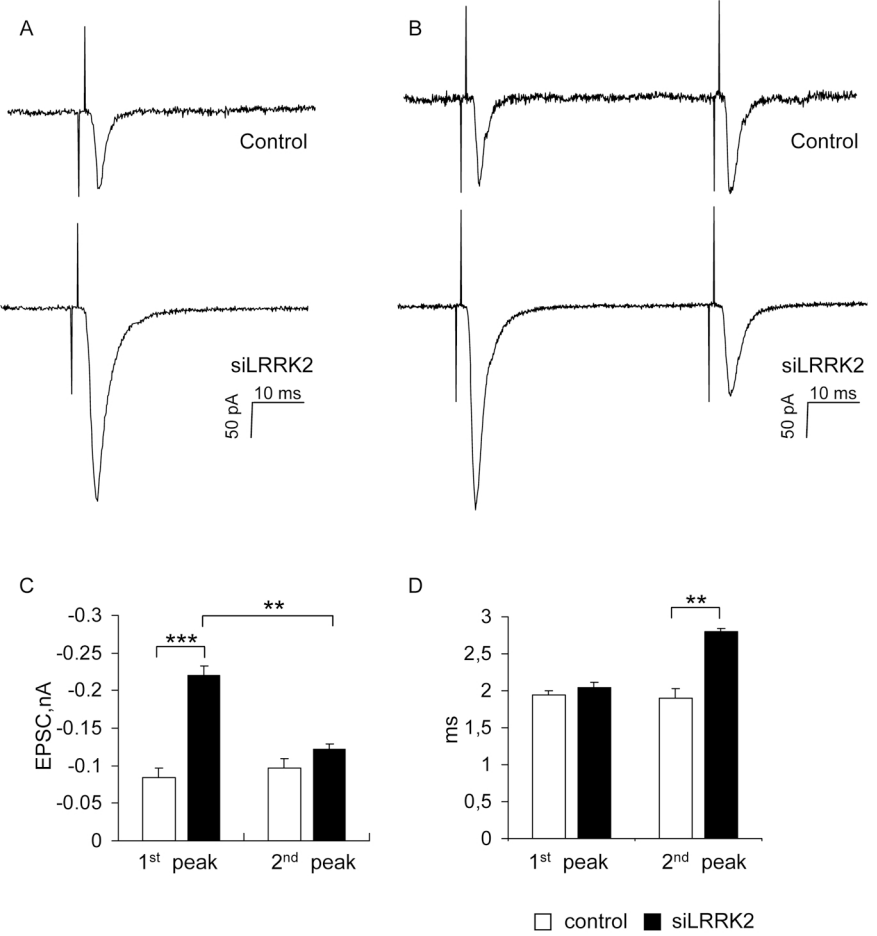
A
Control
siLRRK2
50 pA
10 ms
B
Control
siLRRK2
50 pA
10 ms
C
EPSC,nA
-0.3
-0.25
-0.2
-0.15
-0.1
-0.05
0
***
**
1st peak
2nd peak
D
ms
3
2,5
2
1,5
1
0,5
0
**
1st peak
2nd peak
control
siLRRK2

Figure 2

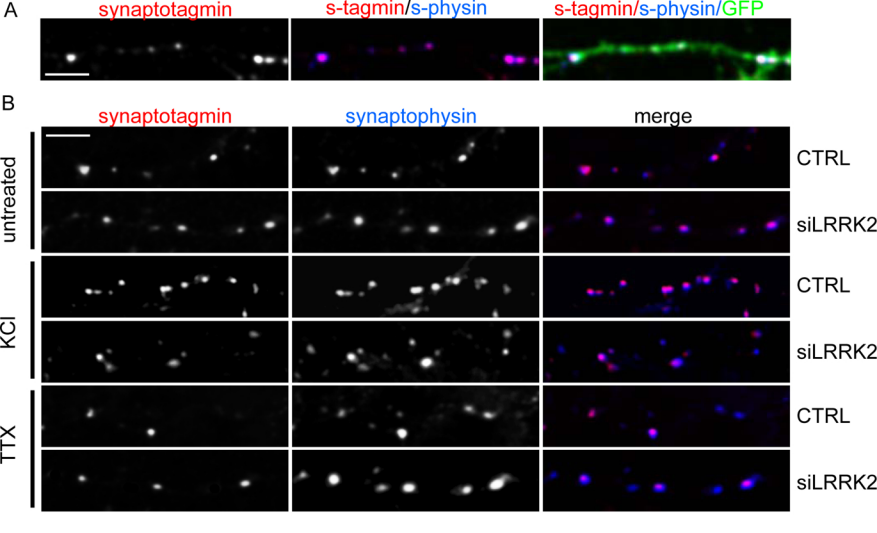
A
synaptotagmin
s-tagmin/s-physin
s-tagmin/s-physin/GFP
B
synaptotagmin
synaptophysin
merge
untreated
KCl
TTX
CTRL
siLRRK2
CTRL
siLRRK2
CTRL
siLRRK2

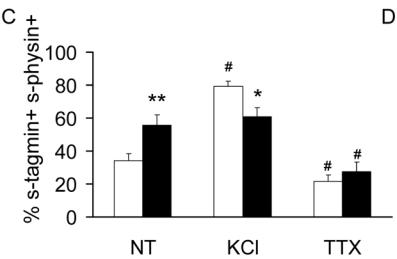
C
% s-tagmin+ s-physin+
100
80
60
40
20
0
**
#
*
#
#
NT
KCl
TTX

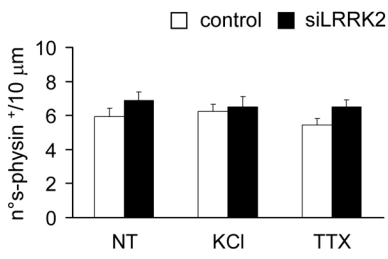
D
control
siLRRK2
n°s-physin +/10 µm
10
8
6
4
2
0
NT
KCl
TTX

Figure 3

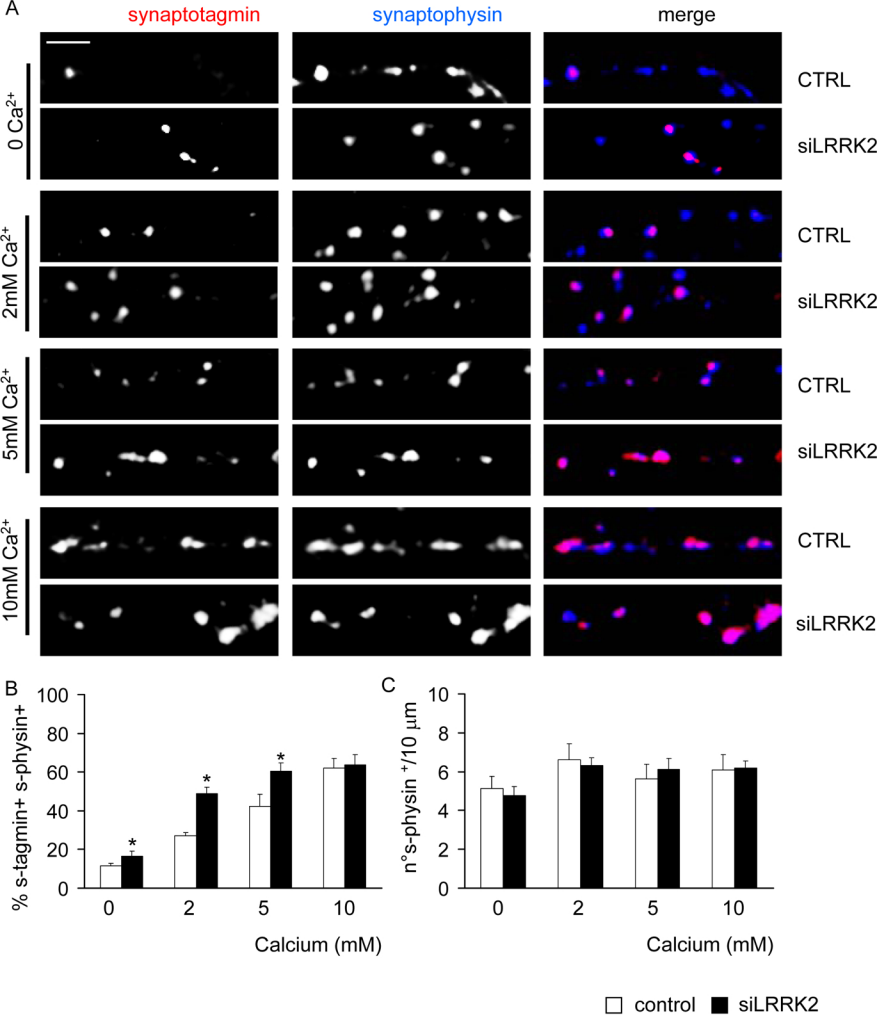
A
synaptotagmin
synaptophysin
merge
0 Ca2+
2mM Ca2+
5mM Ca2+
10mM Ca2+
CTRL
siLRRK2
B
% s-tagmin+ s-physin+
Calcium (mM)
C
n°s-physin +/10 µm
Calcium (mM)
control
siLRRK2

Figure 4

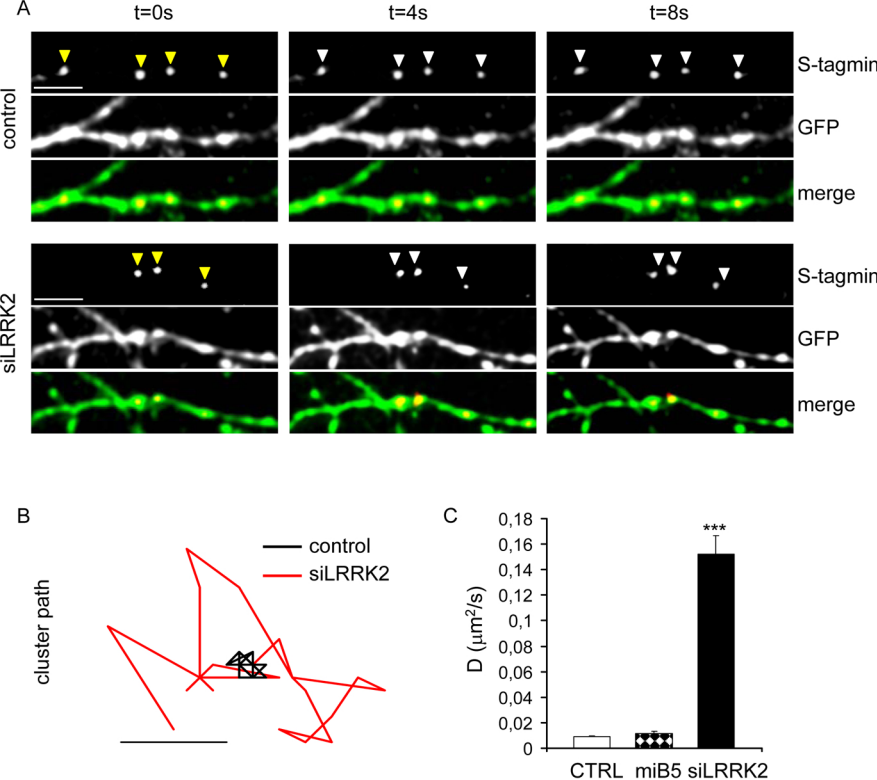
A
t=0s
t=4s
t=8s
control
S-tagmin
GFP
merge
siLRRK2
S-tagmin
GFP
merge
B
cluster path
control
siLRRK2
C
D (µm²/s)
0,18
0,16
0,14
0,12
0,1
0,08
0,06
0,04
0,02
0
***
CTRL
miB5
siLRRK2

Figure 5

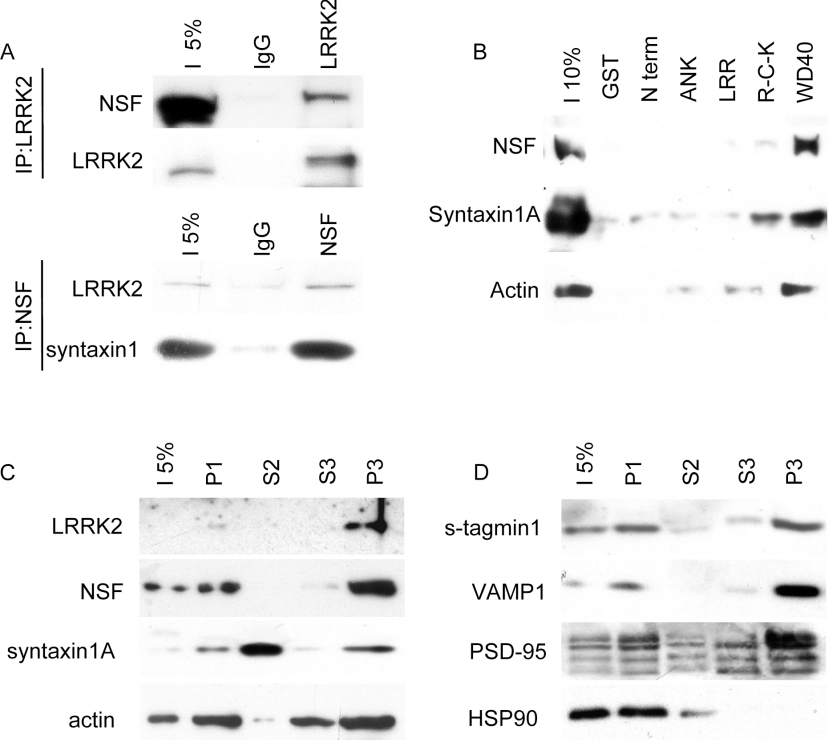
A
I 5%
IgG
LRRK2
IP:LRRK2
NSF
LRRK2
I 5%
IgG
NSF
IP:NSF
LRRK2
syntaxin1
B
I 10%
GST
N term
ANK
LRR
R-C-K
WD40
NSF
Syntaxin1A
Actin
C
I 5%
P1
S2
S3
P3
LRRK2
NSF
syntaxin1A
actin
D
I 5%
P1
S2
S3
P3
s-tagmin1
VAMP1
PSD-95
HSP90

Figure 6

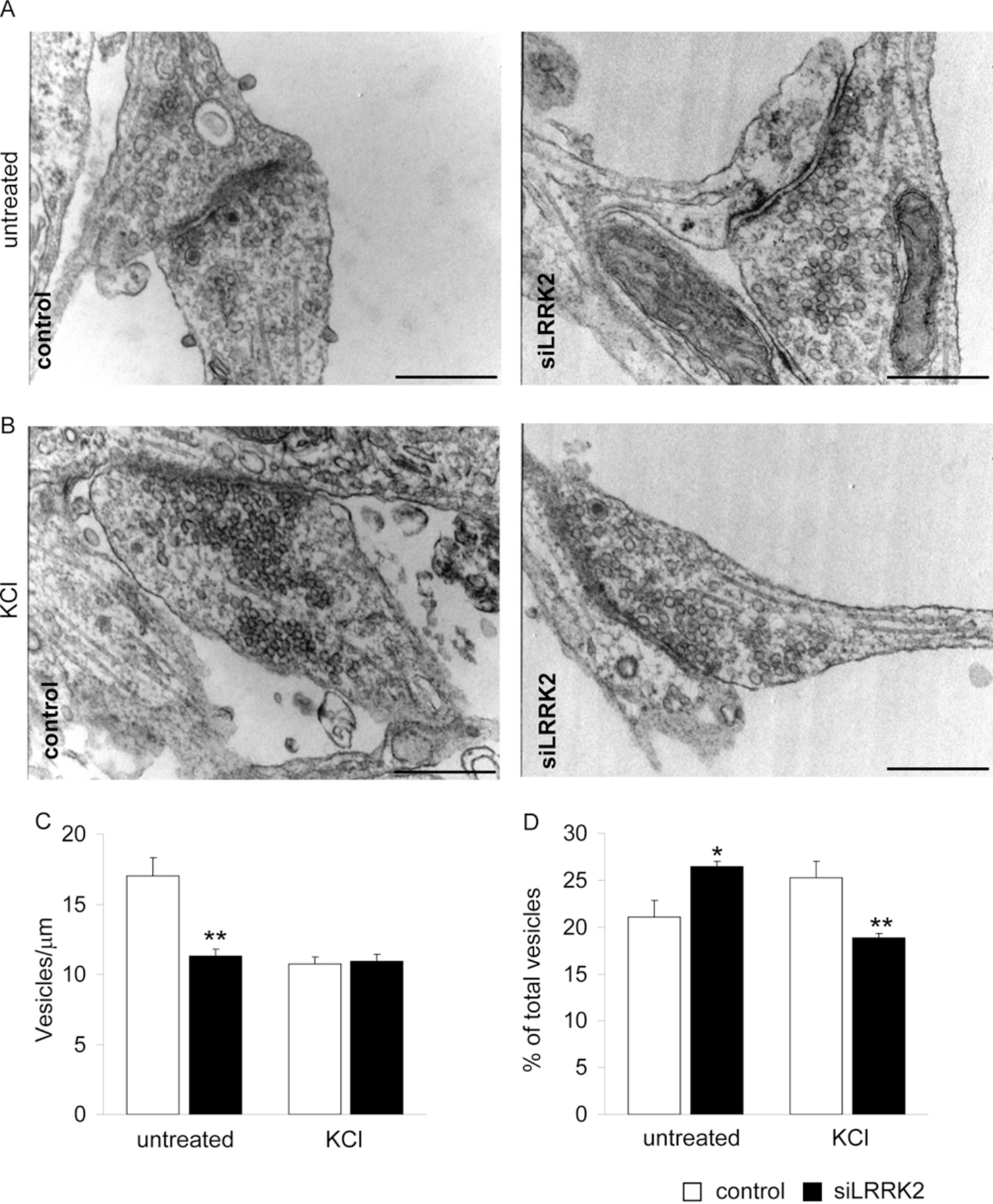
A
untreated
control
siLRRK2
B
KCl
control
siLRRK2
C
Vesicles/µm
20
15
10
5
0
**
untreated
KCl
D
% of total vesicles
30
25
20
15
10
5
0
*
**
untreated
KCl
control
siLRRK2

Figure 7

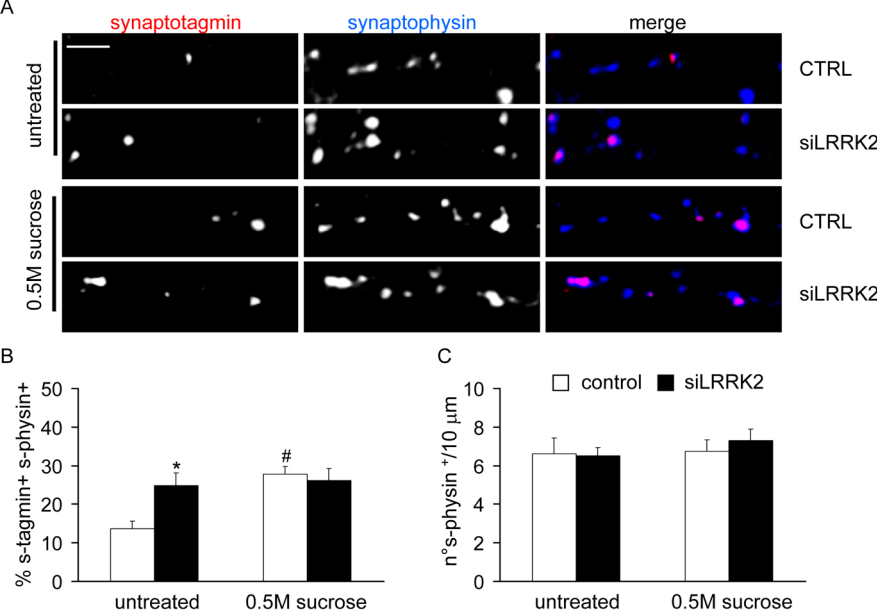
A
synaptotagmin
synaptophysin
merge
untreated
0.5M sucrose
CTRL
siLRRK2
CTRL
siLRRK2
B
% s-tagmin+ s-physin+
50
40
30
20
10
0
*
#
untreated
0.5M sucrose
C
control
siLRRK2
n°s-physin +/10 µm
10
8
6
4
2
0
untreated
0.5M sucrose

Figure 8

Identified Proteins	Accession	MW	N° peptides	Domain	Function
Alpha-actin-2	P62737	42 kDa	10	WD40	Component of cytoskeleton
AP-1 complex subunit beta-1	O35643	104 kDa	8	WD40	Required for vesicle sorting during endocytosis
AP-2 complex subunit alpha-1	P17426	108 kDa	5	WD40	AP-2 complex is a hetero-tetramer; it mediates the recruitment of clathrin to membranes and plays a role in the recycling of synaptic vesicle membranes from the pre-synaptic surface
AP-2 complex subunit alpha-2	P17427	104 kDa	7	Ank	
AP-2 complex subunit beta-1	Q9DBG3	105 kDa	5	WD40	
Calcium-dependent secretion activator 1	Q80TJ1	153 kDa	3	WD40	Calcium-binding protein involved in the exocytosis of synaptic vesicles
Clathrin coat assembly protein AP180	Q61548	92 kDa	6	WD40	Components of the adapter complex which links clathrin to coated vesicles
Clathrin heavy chain 1	Q68FD5	192 kDa	52	WD40	Main coat of coated pits and vesicles
Dynamin-1	P39053	97 kDa	27	WD40	Microtubule-associated protein involved in endocytosis of vesicles
Synapsin-1	O88935	74 kDa	4	WD40	Neuronal phosphoprotein that coats synaptic vesicles
Synaptic vesicle glycoprotein 2A	Q9JIS5	83 kDa	5	WD40	Regulates vesicle fusion by maintaining the readily releasable pool
Syntaxin 1B	P61264	33 kDa	5	WD40	Involved in docking of synaptic vesicles at presynaptic active zones
Vesicle-fusing ATPase	P46460	83 kDa	21	WD40	Required for vesicle-mediated transport

Table 1 LRRK2 interactors. A domain based GST-pull down approach was performed to explore LRRK2 interactome. GST fusion proteins covering full length LRRK2 and mimicking its functional domain (GST-N-term, GST-ANK, GST-LRR, GST-R-C-K, GST-WD40) was used to retain interactors from adult mouse brain lysate. The nature of the pulled proteins including putative interactors was identified by LC-MS/MS. Peptide identifications were accepted if they could be established at greater than 95%, while protein identifications were accepted if they could be established at greater than 99% probability and contained at least 2 identified unique peptides. Only hits confirmed by more then 2 independent experiments and absent in the GST control sample were taken in consideration. The table reports protein name, UniProtKB/Swiss-Prot accession number, protein molecular weight, number of unique peptides identifying the indicated protein, GST-fusion domain bound and protein putative function as annotated in UniProt database. Supplementary Table 1 reports additional peptides information.